Received: 14 February 2022 | Revised: 16 May 2022 | Accepted: 24 June 2022

DOI: 10.1002/pro.4384

FULL-LENGTH PAPER

THE PROTEIN SOCIETY WILEY

A method for quantifying how the activity of an enzyme is affected by the net charge of its nearest crowded neighbor

Jordan C. Koone | **Chad M. Dashnaw** | **Mayte Gonzalez** | **Bryan F. Shaw**

Department of Chemistry and Biochemistry, Baylor University, Waco, Texas, USA

Correspondence
Bryan F. Shaw, Department of Chemistry and Biochemistry, Baylor University, Waco, TX 76706, USA.
Email: bryan_shaw@baylor.edu

Funding information
National Science Foundation, Grant/Award Number: CHE: 2203441; Welch Foundation, Grant/Award Number: AA-1854

Review Editor: Aitziber Cortajarena

Abstract

The electrostatic effects of protein crowding have not been systematically explored. Rather, protein crowding is generally studied with co-solvents or crowders that are electrostatically neutral, with no methods to measure how the net charge (Z) of a crowder affects protein function. For example, can the activity of an enzyme be affected electrostatically by the net charge of its neighbor in crowded milieu? This paper reports a method for crowding proteins of different net charge to an enzyme via semi-random chemical crosslinking. As a proof of concept, RNase A was crowded (at distances ≤ the Debye length) via crosslinking to different heme proteins with $Z = +8.50 \pm 0.04$, $Z = +6.39 \pm 0.12$, or $Z = -10.30 \pm 1.32$. Crosslinking did not disrupt the structure of proteins, according to amide H/D exchange, and did not inhibit RNase A activity. For RNase A, we found that the electrostatic environment of each crowded neighbor had significant effects on rates of RNA hydrolysis. Crowding with cationic cytochrome c led to increases in activity, while crowding with anionic "supercharged" cytochrome c or myoglobin diminished activity. Surprisingly, electrostatic crowding effects were amplified at high ionic strength ($I = 0.201$ M) and attenuated at low ionic strength ($I = 0.011$ M). This salt dependence might be caused by a unique set of electric double layers at the dimer interspace (maximum distance of 8 Å, which cannot accommodate four layers). This new method of crowding via crosslinking can be used to search for electrostatic effects in protein crowding.

KEYWORDS
chemical crosslinking, enzyme kinetics, macromolecular crowding, RNase A

1 | INTRODUCTION

Electrostatic interactions help drive the binding and polarization of substrates during enzyme catalysis.[1–5] With some enzymes, the internal electric field at or near the active site appears to lower ΔG by polarizing the substrates.[6,7] These effects can be large and occur over long distances: the internal electric field at the active site of ketosteroid isomerase lowers the free energy barrier of the rate determining step by up to 7 kcal/mol.[8]

Studies of these electrostatic effects in enzyme catalysis are typically probed by *intramolecular* changes in

charge or hydrophobicity, via site directed mutagenesis or by changing ionic strength of solvent.[8–10] Less is known regarding *intermolecular* electrostatic forces in a crowded environment. That is, how do the electric fields (or net charge) of neighboring proteins impact enzymatic activity? Such intermolecular electrostatic effects of protein crowding, if substantial, would not only be relevant to understanding protein localization and cellular function, but also cellular death.[11–13] During apoptosis, crowding increases 10-fold and the concentration of intracellular ions (that screen long range electrostatic interactions) decreases threefold.[11,14,15]

Studies of protein crowding have focused on measuring how electrostatically neutral crowders affect enzymatic activity, protein structure, and protein stability.[16–20] These studies show that crowding can have diverse effects on enzyme activity (increasing or decreasing activity, or a null effect).[21–27] These studies do not address long range intermolecular electrostatic effects by crowders. We cannot find any studies that measured how the net charge (Z) of a protein "neighbor" affects the activity of an enzyme in a crowded environment. Considering the importance of electrostatic effects in catalysis, and the long range over which coulombic interactions occur (~10 Å through buffer at $I = 0.1$ M, but further in the ion-free hydrophobic interior of crowded proteins), it seems long past time to find simple ways to begin to investigate how the activity of an enzyme might be affected by the net charge of its nearest neighbor.

In this proof of concept paper, we describe a new general method to study how the net charge of a protein affects the activity of an enzyme during crowding. The model enzyme that we use to test this method, RNase A, is known to have kinetic salt effects, with k_{cat}/K_m decreasing 100-fold as salt concentration is increased 20-fold.[28,29] Salt effects for RNase A are buffer-specific, as some buffers contain a charged impurity that inhibits RNase A more strongly at low than high salt.[30] Although these salt effects remain poorly understood,[30–33] this effect suggests that long range electrostatic forces might be important in the binding and/or catalytic hydrolysis of RNA by RNase A.

The RNase A enzyme possesses two catalytically important histidine residues (H12 and H119) with pK_a's of ~5.8 and 6.3, respectively (Scheme 1).[34–36] Previous studies by Raines et al. have described how electrostatic control of His119 by Asp121 enables RNase A to protonate the 3′ ribose group of RNA during the transphosphorylation step.[34–36] Here, the pK_a of H12 and H119 are depressed by nearby lysine residues.[37] These Lys-His coulombic interactions are screened by salt.[37] We hypothesize that the activity of RNase A might be perturbed by the electric field of a crowded protein via "charge regulation"[29,38–41] of these two histidine residues, inter alia. In addition, RNase A has discrete sites that help electrostatically align RNA to facilitate selective hydrolysis at pyrimidine nucleotides.[41,42] One subsite, B1, is composed of Thr45, Asp83, Phe120, and Ser123 which utilize

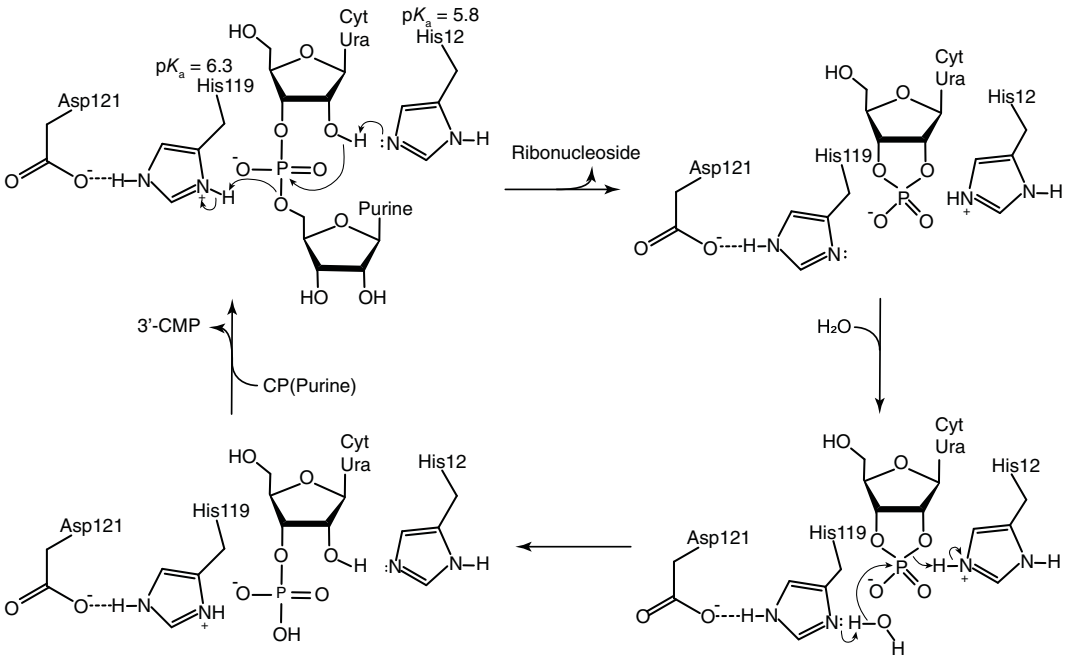

SCHEME 1 Mechanism of RNA hydrolysis by RNase A.

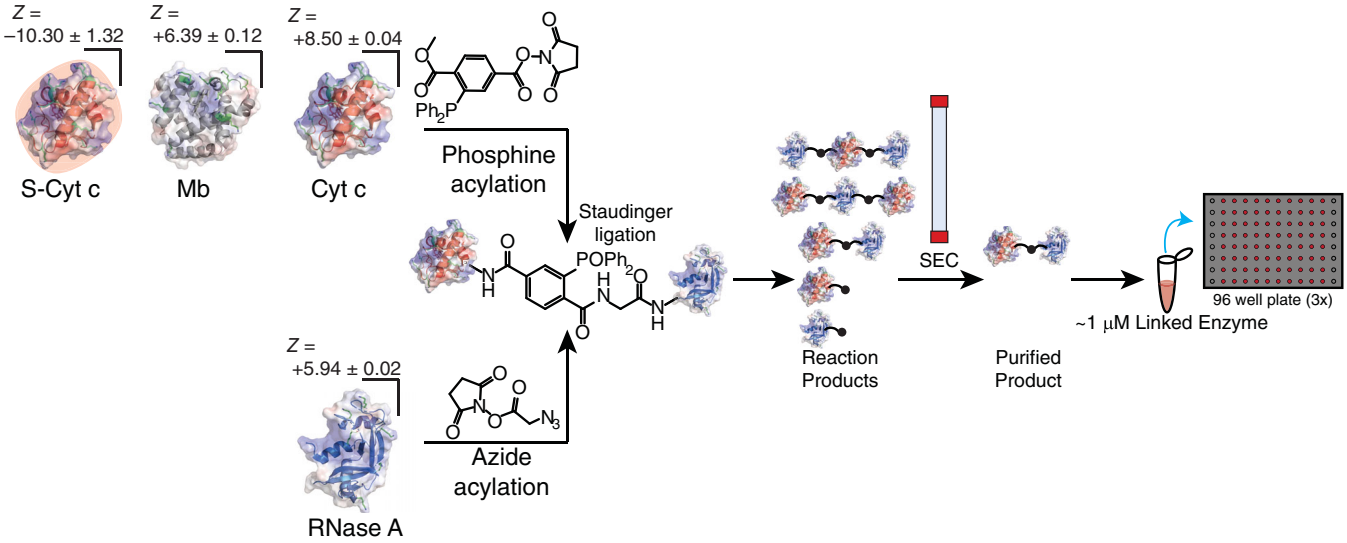

SCHEME 2 Mimicking protein crowding by semi-random Staudinger ligation of a protein crowder (with a specific net charge, Z) to the RNase A enzyme. The Staudinger-linked heterodimer (a polydisperse mixture of geometric dimers) can be purified from monomers or higher order complexes.

hydrogen bonding and van der Waals forces to selectively bind only pyrimidine bases.[42–44] There are, of course, additional mechanisms by which such crowding can affect activity that are electrostatic in nature.[45,46]

This current study expands upon a recently reported method of semi-random chemical crosslinking to mimic the crowding of proteins by other proteins.[47] Although crosslinking is widely used to trap specific protein–protein interactions,[48–51] we found that commercial crosslinkers can link noninteracting proteins (of various net charge) in a quasi-random fashion.[47] This semi-random crosslinking method allows us to eliminate possible site-specific electrostatic effects that might arise from a genetically engineered fusion protein.[47] Once proteins are crosslinked (into heterodimers) enzymatic activity assays can be performed to test for kinetic neighbor effects. In this study, RNase A was crowded with cytochrome c (Cyt c), myoglobin (Mb), and supercharged (anionic) Cyt c (denoted S-Cyt c). These heme proteins were chosen as ideal crowders because their visible chromophore permits accurate quantitation of the RNase–Cyt c complex and the RNase–Mb complex, which is necessary for quantitation of K_M, k_{cat}, and V_{max}.

2 | RESULTS AND DISCUSSION

As a proof of concept, RNase A was linked to either positively charged Cyt c, positively charged Mb, or negatively charged ("supercharged") Cyt c at a maximum linker distance of 7.9 Å. S-Cyt c was prepared by polycarboxylating wild-type Cyt c via succinic anhydride.[52] The heterobifunctional Staudinger linkers that we use (Scheme 2) allow us to generate only heteromeric species. These linkers are not necessarily selective to a particular lysine residue but create a polydisperse set of linkages.[53]

There are two reasons that we acylated/percarboxylated Cyt c (to generate "S-Cyt c") to model the effects of negatively charged proteins, as opposed to linking an entirely different protein that is as negatively charged as S-Cyt c. First, the simplest way to alter the surface charge of a protein, without altering its sequence or shape (and only minimally altering its structure) is to acylate surface lysine residues.[10,52,54] Although lysine acylation can lower the thermostability of a protein (in most, but not all cases),[55] the resulting proteins can have similar structures according to circular dichroism, amide H/D exchange, and X-ray crystallography.[54] Second, we cannot find any commercially available heme protein—let alone any naturally occurring heme protein—that has a high net negative charge at pH 5.0, that is, $Z \geq |-10|$.

Crosslinking resulted in formation of heterodimers and trimers, in addition to low-abundance higher order oligomers (Figure 1). We were initially interested in measuring the RNase A activity of trimers and higher order oligomers, but we bypassed their analysis for two reasons. First, the protein stoichiometry of any trimeric or higher order species would be unverifiable. For example, a trimeric species eluting at 40 kDa in the size exclusion column (or migrating at 40 kDa on sodium dodecyl sulfate–polyacrylamide gel electrophoresis [SDS-PAGE]) could be comprised of: (a) a trimer of RNase A linked to two Cyt c (38.4 kDa) or (b) one Cyt c that is linked to two

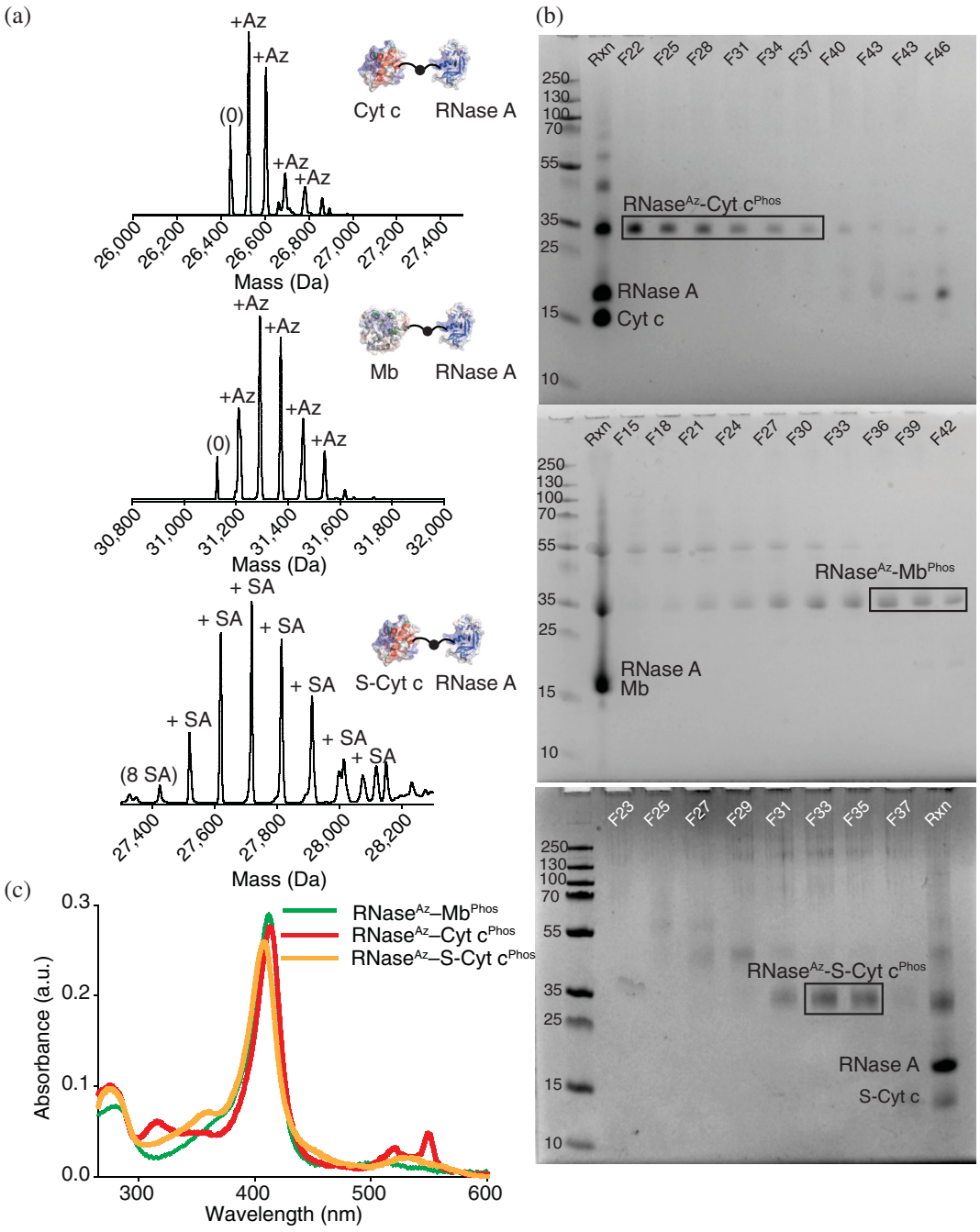

FIGURE 1 (a) Deconvoluted mass spectra and (b) sodium dodecyl sulfate–polyacrylamide gel electrophoresis of purified heterodimeric proteins of RNase^{Az}–Cyt c^{Phos} (top) RNase^{Az}–Mb^{Phos} (middle), and RNase^{Az}–S-Cyt c^{Phos} (bottom). (c) UV-vis spectra of purified dimers ($\lambda_{max} = 408$ nm for Cyt c and S-Cyt c heme and 410 nm for Mb heme)

RNase A (39.7 kDa). While this latter trimer should be minimized by limiting amounts of phosphine linker on each Cyt c, any small amount would skew RNase A concentrations. Second, the low crosslinking yield results in trace amounts of higher order oligomers.

To determine the actual net charge (denoted Z_{CE}) of each protein before crosslinking, protein "charge ladders"[52,56] were synthesized and separated by capillary electrophoresis (CE) (Figure 2). These ladders are only used for determining the charge of the protein before crosslinking and are not subsequently used in crosslinking. Briefly, lysine-ε-NH_3^+ groups in RNase A, Mb, and Cyt c were acetylated with acetic anhydride. This acetylation causes a change in charge of approximately 0.9 units per modification. The net charge of each protein is determined by extrapolating the *x*-intercept of the plot of mobility of each "rung" versus the number of acetylated lysines (*N*). The *x*-intercept equals the quotient of the net

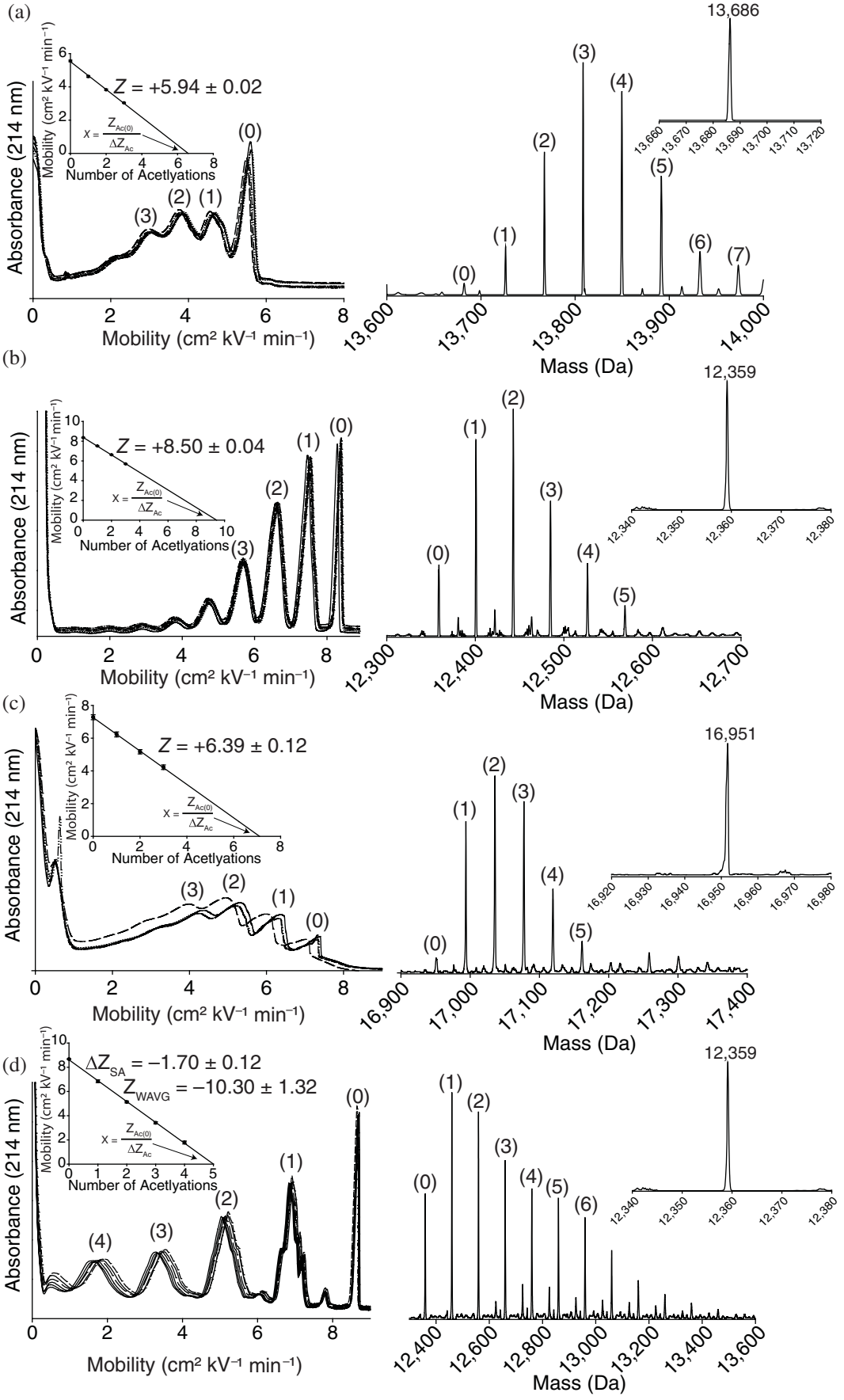

FIGURE 2 Legend on next page.

charge of the unmodified protein, Z_{CE} (the zeroth rung of the charge ladder) and the change in charge of acetylation (ΔZ_{Ac}). The net charge for RNase A, Cyt c, Mb, and S-Cyt c were determined at pH 5.0 (Figure 2).

With these values, the question immediately arises: How does RNase A (Figure 2a, $Z_{CE} = +5.94 \pm 0.02$) adjust its electrostatic environment when linked to a protein neighbor such as Cyt c (Figure 2b, $Z_{CE} = +8.50 \pm 0.04$), Mb (Figure 2c, $Z_{CE} = +6.39 \pm 0.12$), or S-Cyt c (Figures 2d and S1, $Z_{CEWAVG} = -10.30 \pm 1.32$)? This issue—the magnitude by which two proteins affect each other's net charge in a crowded environment—is poorly understood.[57–59] The question has been examined with Monte Carlo simulations[60] and protein charge ladders.[47] Lund and Jonsson simulated how the net charge of calbindin and lysozyme change as they approach each other at a distance of ~25 Å (mass center to mass center) and ionic strength of $I = 0.006$ M (pH 4.0). Lysozyme was predicted to regulate its charge from +9.3 to +9.5 and calbindin from +1.5 to −0.5.[57,61] These changes in charge are attributed to the shift in pK_a's of ionizable residues in each protein in response to the new electrostatic environment created by the neighboring protein.

Using protein "charge ladders" and chemical crosslinking, we recently found that this type of charge regulation was small for a particular pair of proteins (Mb and α-lactalbumin) at $I = 0.025$ M.[47] However, larger effects might be observed at lower ionic strength (e.g., at $I < 0.01$ M), which might be physiologically relevant in membrane interiors or during liquid–liquid phase separation.[62,63] Nevertheless, how any of these changes in pK_a's of ionizable residues—large or small—might impact enzymatic activity in vitro has not been measured or investigated (to our knowledge).

Analysis of monomers and heterodimers with CE and protein "charge ladders" could, in theory, determine how the net charge of proteins change upon crowding/linking.[47] We analyzed a protein charge ladder of the heterodimer (RNase^{Az}–Cyt c^{Phos}) with CE (Figure S1). Unfortunately, the dimeric ladder is poorly resolved (Figure S1). However, interpolation of these poorly resolved peaks yielded a $Z_{CE} = +12.58 \pm 0.35$ for the heterodimer (Figure S1). This net charge is nearly identical to $Z_{formal} = +13.09 \pm 0.04$, that is, the sum of the net charges of RNase A (Figure 2a, $Z_{CE} = +5.94 \pm 0.02$) and Cyt c monomers (Figure 2b, $Z_{CE} = +8.50 \pm 0.04$), when correcting for Staudinger crosslinking at two lysine (previously measured to be $\Delta Z = -1.34$).[47]

Mass spectrometry (MS) was used to assess the extent of modification of lysine in each protein with its bifunctional linker before mixing and crosslinking (Figure S2; Az = 83 Da, PPh_3 = 346 Da). Our goal was to only attach between 1 and 3 linkers to each protein. Note that there was at most three to four additional acyl-azide modifications (WAVG = 3.22) present on the heterodimers, according to MS (Figure 1a). Modified proteins were then mixed at 4°C (for at least 24 hr) to form the heteromeric Staudinger linkages between RNase A and either Cyt c, Mb, or S-Cyt c. After isolation of heterodimers with size exclusion chromatography (SEC), the purity was assessed with MS and SDS-PAGE (Figure 1a,b). UV-vis spectroscopy confirmed that the heme was still present in all linked proteins (Figure 1c).

Liquid chromatography (LC)-MS/MS of tryptic digests of Az and PPh_3 modified (but unlinked) proteins suggested that each linker attached nonselectively to different lysines in RNase A (Figures 3, 4, and S3), Mb (Figures 3 and S4), and Cyt c (Figures 4 and S5). We did not detect any modified histidine residues, as expected. Both Az and PPh_3 linking reagents modified at least ~60% of lysine residues (for RNase A^{Az}: K31, K41, K61, K91, K98, and K104; Cyt c^{Phos}: K8, K9, K14, K23, K26, K28, K40, K87, K88, K89, and K100; Mb^{Phos}: K42, K45, K47, K50, K62, K63, K79, K87, K96, K98, and K102). It is likely that Az and PPh_3 reagents modified additional lysines that were not detected in MS/MS.

The results of nonselective acylation are supported by previous studies showing that small molecule acylating agents (e.g., anhydrides, N-hydroxysuccinimide [NHS]-esters, and aryl esters) acylate lysine in proteins semi-randomly.[47,64–66] Even partially buried lysine residues are reactive with small organic molecules, because these lysines can associate with amphiphilic/hydrophobic molecules (in some cases, more so than solvent accessible lysine residues).[67] The heterodimers produced are likely to be a polydisperse mixture of multiple geometric dimers between RNase A and Mb, Cyt c, or S-Cyt c. We expect that after acylation of 9–15 lysine residues, the attachment of the linker to S-Cyt c would still produce a polydisperse mixture following attachment of phosphine linker.

FIGURE 2 Using lysine-acyl "protein charge ladders" to determine the net charge of all proteins used in this study, in their native, solvated state. Replicate electropherograms (left) and mass spectra (right) of (a) RNase A, (b) Cyt c, and (c) Mb modified with acetic anhydride (AA). The *x*-intercept equals the net charge (Z) of the unmodified protein divided by the change in charge associated with lysine acetylation (ΔZ_{Ac}). (d) Cytochrome c was supercharged by acylation with succinic anhydride, to yield "supercharged" Cyt c (denoted S-Cyt c). This plot determines the change in charge of each succinylation (ΔZ_{SA}), at pH 5.0, not the net charge of the protein (which is determined by multiplying ΔZ_{SA} by n). In a–d, error bars represent the SD of five replicates

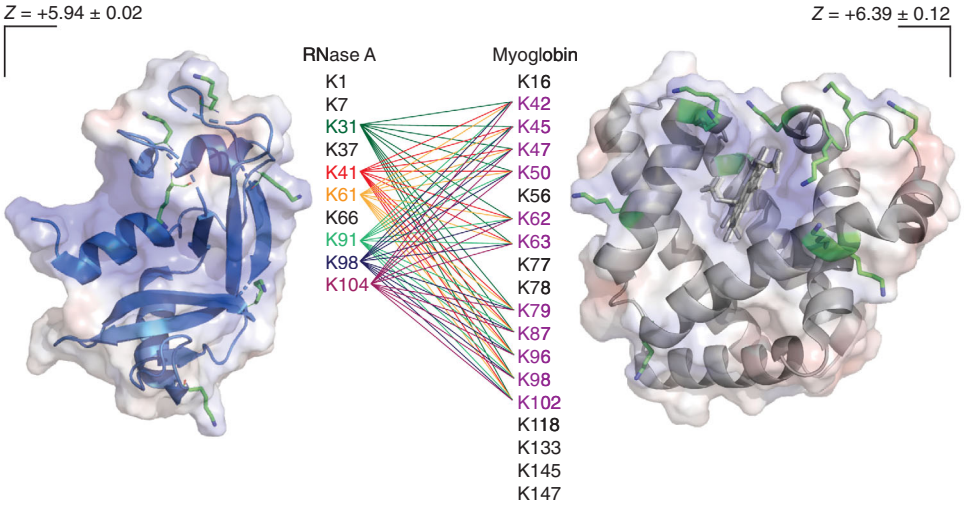

FIGURE 3 Lysine residues of RNase A modified with azide linker and lysine in Mb modified with phosphine linker (shown in colored text). Lines represent the potential crosslinks between each protein upon Staudinger ligation

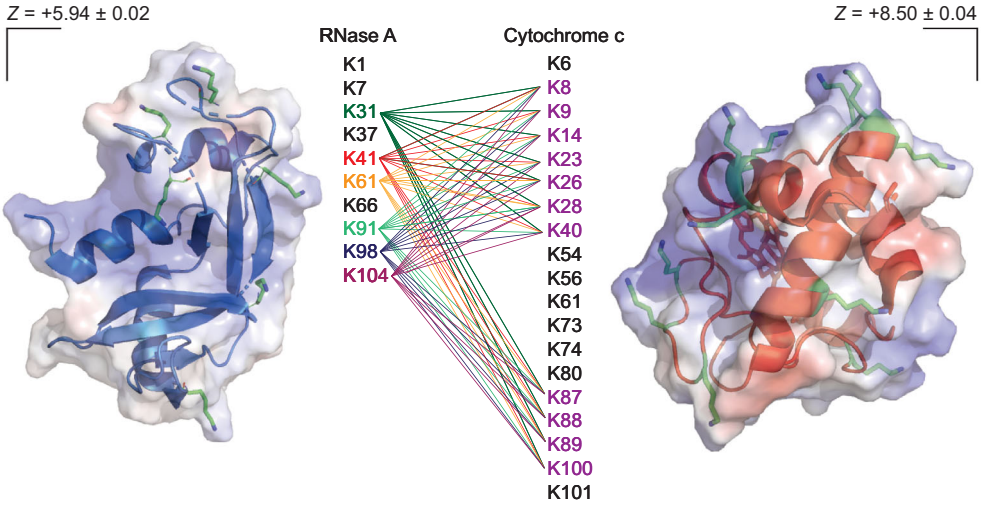

FIGURE 4 Lysine residues of RNase A modified with azide linker and lysine in Cyt c modified with phosphine linker (shown in colored text). Lines represent the potential crosslinks between each protein upon Staudinger ligation

Amide hydrogen/deuterium exchange (H/D exchange)—MS confirmed that the hydrophobic cores of RNase A, Cyt c, and Mb were not affected by acylation with linkers, subsequent crosslinking, or acylation with succinic anhydride in the case of S-Cyt c (Figure 5a, Table S1). Note that the acylation of Cyt c with succinic anhydride (to form S-Cyt c) decreased the rate of amide H/D exchange in 90% D_2O, that is, increased the number of unexchanged hydrogens after 60 min (with a back exchange rate of 43%). This decreased rate of exchange might suggest that acylation tightens the structure of Cyt c to be more solvent inaccessible, but this interpretation is likely inaccurate. Rather, this inverse effect of lysine acylation on the rate of H/D exchange is likely an electrostatic artifact. This kinetic effect is thought to be due to the stabilization of the anionic amide intermediate that forms during base-catalyzed amide H/D exchange, by the amino group of lysine.[31,68] Neutralization of the amino group in lysine, via acylation, abolishes this stabilization and slows the rate of H/D exchange. This effect has been reported for several proteins (including carbonic anhydrase II, superoxide dismutase, Mb, and α-lactalbumin) modified with several types of neutral and anionic acyl groups.[31,47,65,68,69] These reports show that acylation of lysine decreases the rate of amide H/D exchange, while also lowering the thermostability of the protein.

We also point out that the total number of unexchanged hydrogens from each dimer (RNase A^{Az}–Mb^{Phos}: 64.2 ± 11.7 hydrogens; RNase A^{Az}–Cyt c^{Phos}: 50.2 ± 11.0 hydrogens) is within error of the sum of monomers (RNase $A^{Az(1)}$ + $Mb^{Phos(1)}$: 69.7 ± 5.3 hydrogens; RNase $A^{Az(1)}$ + Cyt $c^{Phos(1)}$: 37.1 ± 5.1 hydrogens). This suggests that the linking of any of the three proteins to RNase A did not perturb any of their hydrophobic cores. Isotopic exchange was measured in 90% D_2O at pH 7.5, 22°C. Mass spectra were obtained at three separate conditions: (a) 100% H_2O, 22°C, (b) after 60 min in 90% D_2O, 22°C, and (c) thermally denatured in 90% D_2O, 90°C. The spectrum for each was deconvoluted using three different charge states of monomer or dimer (Figure 5b and

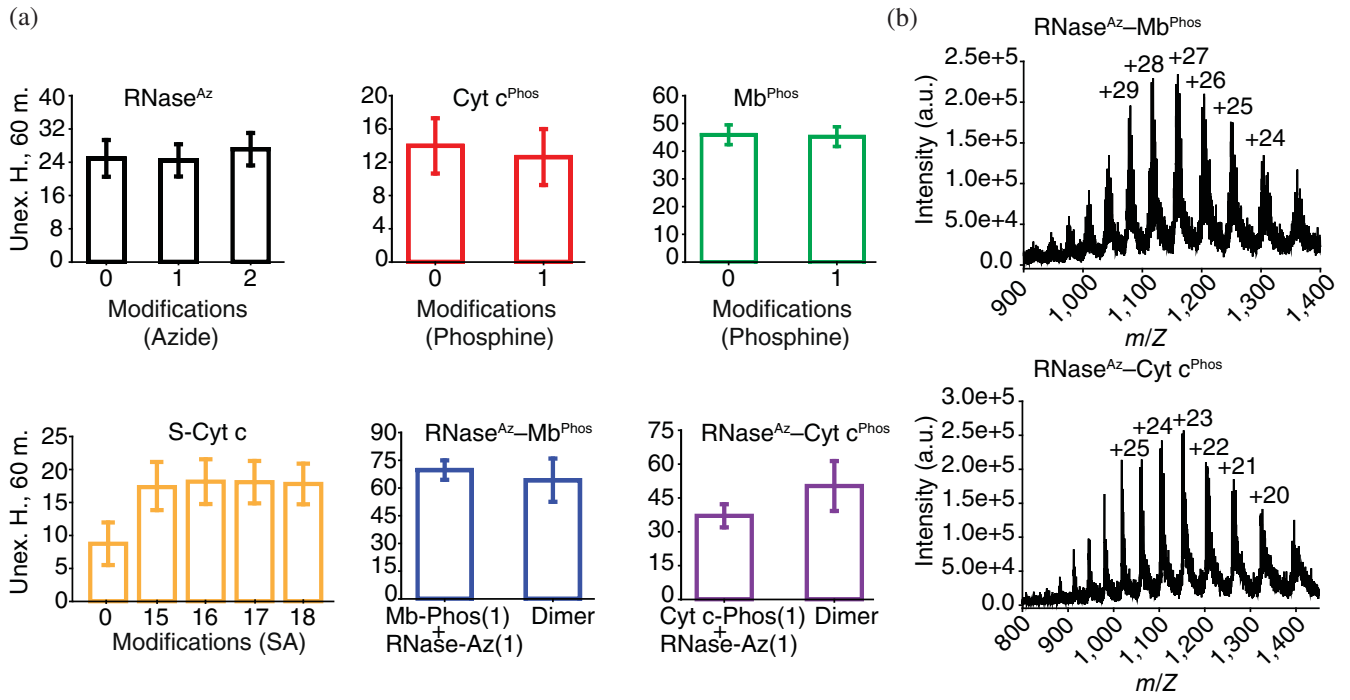

FIGURE 5 (a) H/D exchange of RNase^{Az}, Cyt c^{Phos}, Mb^{Phos}, S-Cyt c, and RNase A linked to either Mb or Cyt c. Unexchanged hydrogens express the number of amide hydrogens that do not exchange after 60 min in 90% D_2O, as calculated from the difference in mass of native protein in D_2O after 60 min, and the mass of perdeuterated (heat-denatured) protein. (b) Raw mass spectra of dimeric species in D_2O

Table S1). The number of unexchanged hydrogens after 60 min for unmodified Cyt c^{Phos} (14.0 ± 4.44 hydrogens), Mb^{Phos} (45.9 ± 3.55 hydrogens) is comparable to previous results.[31,70]

Considering the electrostatic artifacts of using amide H/D exchange to assess structural differences in Cyt c and S-Cyt c, we also analyzed S-Cyt c with differential scanning calorimetry (DSC). The melting temperature (T_m) of Cyt c decreased from 83.51 ± 0.18°C to 50.41 ± 0.07°C upon acylation of ~17 lysines with succinic anhydride (Figure S6). The measured T_m of unmodified Cyt c is comparable to previous results[71] (and the diminished thermostability upon acylation is similar in magnitude to decreases observed for other thermostable proteins).[31,47,65,68,69] Examination of the thermogram of S-Cyt c and Cyt c suggests that acylation of as many as ~17 lysine did not increase the amount of unfolded protein at the temperature of the enzyme assays (22°C).

The results of DSC and H/D exchange suggest that although the S-Cyt c protein is less thermostable than Cyt c, the hydrophobic core of S-Cyt c is not disrupted by acylation of up to ~17 lysine with succinic anhydride. We also point out that this seemingly contradictory effect of lysine acylation on the structure of Cyt c—i.e., acylation lowers thermostability but slows amide H/D exchange—has been previously reported for other metalloproteins.[31,65,68] For example, the acetylation of all 18 lysine in carbonic anhydrase II lowers the T_m of the enzyme from ~70 to 50°C, and increases the number of unexchanged hydrogens by ~18.[68] The peracetylated and unacetylated forms of this protein both crystallize with superimposable backbones.[54]

Enzyme assays of modified monomeric and cross-linked RNase A were conducted in a 96 well-plate. Here, 24 technical replicates of each substrate concentration were run to generate statistically meaningful data. Assays were run as previously described using total RNA from *Saccharomyces cerevisiae*. This assay follows the decrease in absorbance of RNA (at 300 nm) upon hydrolysis. RNA has a λ_{max} of 260 nm but is most linear at 300 nm.[72]

The concentration of RNase A and its heterodimers with Mb and Cyt c were determined using molar extinction coefficients of each protein (RNase A ε_{280}: 9,800 M/cm[73]; Cyt c ε_{408}: 101,600 M/cm[74]; and Mb ε_{410}: 188,000 M/cm).[75] Since linked proteins had a visible chromophore, we were also able to quantify the added absorbance of the phosphine linker at 280 nm. The molar extinction coefficient of acyl-phosphine at 280 nm was found to be 3,990 M/cm (Figure S7). Bicinchoninic acid protein assays were used to further verify the concentration of the final dilution of each stock protein used in enzymatic assays (Table S2). Protein concentrations determined by both methods differed on average by 9.9% (Table S2).

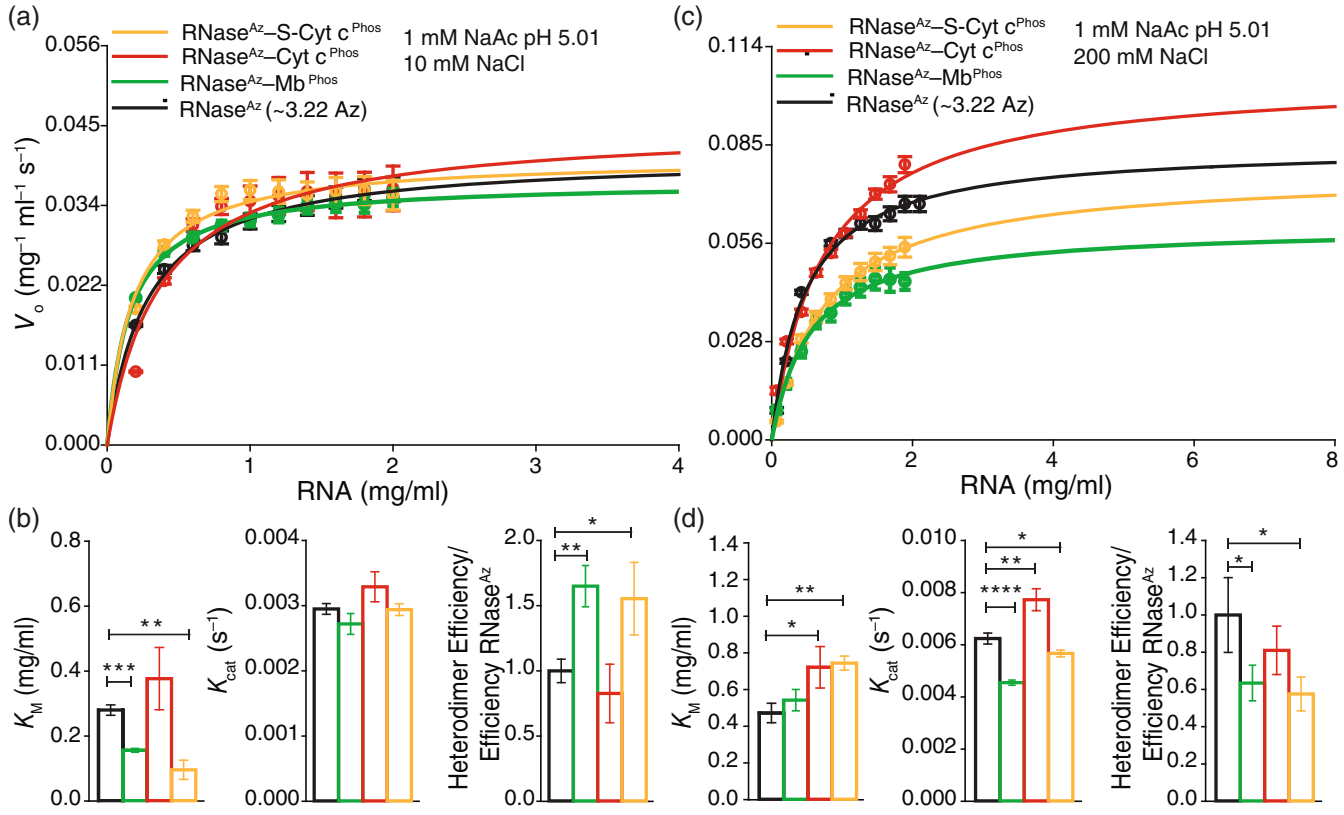

FIGURE 6 Kinetic assays of monomeric and crosslinked RNase A at pH 5.01. Michaelis–Menten plots of RNase^{Az} (black), RNase^{Az}–Mb^{Phos} (green), RNase^{Az}–Cyt c^{Phos} (red), and RNase^{Az}–S-Cyt c^{Phos} (orange) at (a) 1 mM NaAc, 10 mM NaCl, pH 5.01 with (b) extracted kinetic parameters and (c) 1 mM NaAc, 200 mM NaCl, pH 5.01 with (d) extracted kinetic parameters. Each heterodimer was compared to RNase^{Az} with an unpaired *t* test. Significance is reported as: *$p \leq .05$, **$p \leq .01$, ***$p \leq .001$, and ****$p \leq .0001$

The k_{cat} and K_M of each RNase A enzyme (i.e., unlinked RNase^{Az}, RNase A linked to Cyt c or Mb, or S-Cyt c) was quantified at two pH values and buffers: a pH of 5.01, using 1 mM sodium acetate (NaAc) and a pH of 6.02 using 1 mM 2-(*N*-morpholino)ethanesulfonic acid (MES). Two different salt concentrations were used at each pH: 10 mM NaCl ($I = 0.011$) and 200 mM NaCl ($I = 0.201$). In this paper, we largely focus on experiments performed in acetate buffer, pH 5.01. The MES buffer has been shown to contain a anionic contaminant that inhibits activity (oligo[vinylsulfonic acid]).[30,76] We nevertheless performed experiments in this buffer as much of the seminal work on RNase A is carried out in MES.[77–84] The general magnitude of rates of RNA hydrolysis by RNase A are comparable to previous measurements of the free enzyme.[85,86]

Regarding the enzymatic activity of modified RNase A (either linked or unlinked), note that the acylation of Lys41 by the azide linker was detected in RNase A (Figures 3 and 4). Thus, a subpopulation of either type of RNase A (i.e., modified heterodimer or modified monomer) bear modification of Lys41. Previous studies show that Lys41 is necessary for catalysis (the K41R substitution abolishes activity).[29,87] Lysine-41 is thought to stabilize the transition state during transphosphorylation.[29,87,88] Modification of Lys41—which exists in a fraction of the randomly acylated mixture—might inhibit catalysis in the subpopulation bearing that modification. However, these inhibitory effects can be accounted for by simply comparing rates of catalysis by acylated/unlinked RNase A (denoted RNase^{Az}) to acylated/crosslinked RNase A.

Proof that acylation does diminish overall activity can be found by comparing the activity of acylated and unacylated RNase A, unlinked to any protein (Figure S8). Here the acylated unlinked RNase A (denoted "RNase^{Az}" in Figure S8) had lower turnover rates (25–50% lower) than unacylated, unlinked RNase A (denoted "RNase A" in Figure S8). The largest inhibitory effect of acylation was observed at pH 6.02, 200 mM NaCl, 1 mM MES. Therefore, the appropriate comparison groups between linked and unlinked RNase A are: (a) acylated, unlinked RNase A (denoted "RNase^{Az}" in Figures 6 and S9), and (b) acylated, crosslinked RNase A.

Michaelis–Menten plots show the activity of crowded and uncrowded RNase A at pH 5.01 with salt

concentrations of 10 mM NaCl (Figure 6a,b) or 200 mM NaCl (Figure 6c,d). Similar plots for RNase A in MES buffer, pH 6.02 (10–200 mM NaCl) can be found in Figure S9. Values of V_{max} and K_M were derived using initial rates determined as previously described.[89,90] Mass extinction coefficients for each assay condition at 300 nm were generated from serial dilutions of RNA (Table S3 and Figure S10). Because the RNA substrate that we used is a polydisperse mixture of oligonucleotides, we do not express K_M or V_{max} in terms of moles per liter but milligrams per milliliter as previously described.[85,86]

We placed particular focus on comparing kinetic differences of crowding by positively charged Cyt c and negatively charged S-Cyt c. These two Cyt c proteins only differ in surface charge by ~18.8 units (Figure 2b,d). This set of proteins, having similar shape and structure but different surface charge, is particularly useful because the heme chromophore (on which we derive RNase A concentrations) is covalently linked to the Cyt c protein (in Mb, the heme is bound noncovalently).

Compared to the uncrowded, unlinked RNase^{Az} control, crosslinking caused modest (but in some cases statistically significant) decreases in K_M at low ionic strength ($I = 0.011$ M), pH 5.01 (Figure 6a,b). In general, the presence of high salt increased the K_M of all RNase A proteins at pH 5.01, which is rationalized by weaker RNA binding at high salt.[9] The greatest observed decrease in K_M of RNase^{Az} was for S-Cyt c, pH 5.01, 10 mM NaCl (Figure 6b). Here, crowding with negatively charged Cyt c resulted in a twofold decrease in K_M relative to unlinked RNase^{Az} and a fourfold decrease in K_M relative to RNase A linked to positively charged Cyt c (Figure 6b). The effects on K_M at pH 6.02 were smaller and less statistically significant at both ionic strengths (Figure S9). This null effect might be caused (at least partially) by the anionic contaminant in MES buffer that inhibits RNase A activity.[30,76]

With regards to k_{cat}, we find that crowding RNase A with anionic S-Cyt c, cationic Cyt c, or Mb, did not greatly affect the k_{cat} of RNase A at pH 5.01 ($I = 0.011$ M), compared to the RNase^{Az} control (Figure 6a,b). This result suggests that the electric field emanating from the surface of these proteins is not affecting the pK_a of the two catalytically important histidine residues (His12 and His119) in RNase A (or otherwise altering the energy of charged transition states).

In contrast, crowding with cationic Cyt c at higher ionic strength, pH 5.01, $I = 0.201$ M caused a 20% increase in k_{cat} ($p < 0.01$) (Figure 6b–d). Under similar conditions, crowding with S-Cyt c and Mb decreased k_{cat} by 10–20%. Similar decreases in k_{cat} (up to 40%) were observed in MES buffer at pH 6.02, $I = 0.201$ M (Figure S9c,d). These results are counterintuitive, as long-range electrostatic effects are expected to be more pronounced at low ionic strength.

2.1 | Possible mechanisms by which crowding alters activity in high salt

The observation of greater effects of crowding on k_{cat} at higher salt suggest that specific ion-protein and ion-protein-substrate Coulombic interactions are at work,[30] and *not* classical Coulombic interactions between the surfaces of the two proteins that alter the free energy of charged transition states or substrate binding (both of which would be screened at high ionic strength). In the case of RNase^{Az}–Cyt c^{Phos} at pH 5.01 ($I = 0.201$ M) the mechanism by which crowding increases k_{cat} and raises K_M must somehow involve Na^+ and or Cl^-.

The historically poor understanding and complex nature of salt effects on RNase A activity (and proteins in general)[9,30–33] do not lend us a single, obvious explanation involving specific protein-ion effects. However, a consideration of the known effects of ionic strength, and RNase A's surface charge on the structure and function of RNase A can help us speculate on possible mechanisms.

Mechanisms invoking protein stability are likely negligible: millimolar concentrations of NaCl do not destabilize the RNase A protein. The melting temperature (T_m) of RNase A is raised by 4°C as NaCl is raised from 0 to 1 M.[9,91] However, NaCl can lower the activity of RNase A under some conditions.[30] This inhibitory effect might be caused by a combination of weakened binding of RNA to RNase A and salt-induced raising of pK_a of catalytically important His12 and His119, which interact with each other and other charged residues. Previous titrations with nuclear magnetic resonance show that increasing NaCl from 0.018 to 0.142 M increases the pK_a of active site His12 and His119 by ~0.5 unit (from their microscopic values of 5.3/5.7 and 5.5/5.9).[37] This salt-induced protonation is thought to occur by the screening of Coulombic interactions between H12, H119 and Lys7, Arg10, and Lys66. These latter residues depress the pK_a of H12 and H119 in low salt, which helps drive catalysis.[37]

It is possible that cationic Cyt c is coulombically depressing the pK_a of these residues (which are scattered across the surface of RNase A and will be collectively near different crosslink sites). Likewise, negatively charged S-Cyt c would raise the pK_a's and possibly lower activity (which we observe at pH 5.01). Perplexingly, however, these types of Coulombic interactions—if they exist—should be stronger in low salt, not high salt.

2.2 | The electrical double layer in the heterodimer interspace: Two, three, or four layers?

It is important to remember, however, that the surface charge of Cyt c or S-Cyt c is not necessarily encountered, per se, by the RNase A enzyme. Rather each member of the heterodimer likely possesses an electrical double layer of solvated ions (Scheme 3), where the charge of the first inner layer should be opposite in sign but equal in magnitude to the surface potential of the protein, and the outer layer is similar in sign to the surface potential.[92] Each solvated layer is thought to span approximately 3.4 Å.[92] When a protein binds to or aggregates with another molecule, desolvation of these layers occurs at the binding interface. However, the crowded system presented in the current study—two proteins linked with a semi-rigid 7.9 Å linker—poses a unique problem. The linker only allows for two or three layers, that is, not all four layers, to exist at surfaces proximal to the linker and dimer interspace (Scheme 3). If there is an odd number of layers, what will the charge of the third layer be?

We assume that portions of these electric double layers (especially at the crowded interspace) alter the pK_a's of residues in RNase A. These ion-specific effects will not necessarily be dependent on the net charge of the crowder. Previous work has shown that the properties of each electric double layer (e.g., charge density, ion charge, and concentration) can differ from protein to protein, independent of the overall net charge of the protein.[63,93,94] We do not know the exact structure or order of the ion layers in the RNase A/Cyt c/Mb crowded systems and whether the second layer does or does not reflect the net surface charge of the protein (Scheme 3). The unique ion layers might be affecting catalysis, possibly by altering the pK_a's of important residues or stabilizing/destabilizing a charged or polar intermediate.

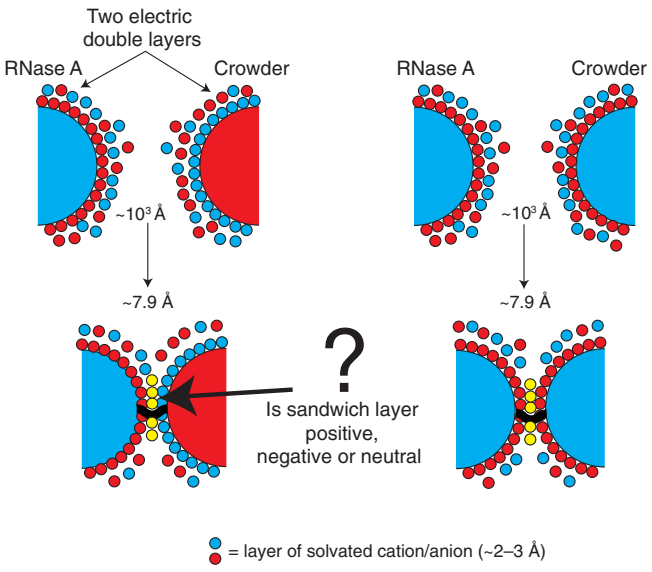

SCHEME 3 Two is company, three is a crowd? Uncrowded proteins (separated by ~200 nm at 0.2 μM) possess an electric double layer of solvated ions. However, all four layers (d = ~3.4 Å per layer) cannot be accommodated at the dimer interspace when crowded at ~8 Å with a crosslinker. How does the charge and concentration of ions in this double/triple layer influence the electrostatic environment? Bulk solvent is depicted with white space; linker is black; layer in question is colored yellow.

3 | CONCLUSION

This method paper demonstrated that the electrostatic crowding of an enzyme by proteins of vastly different net charges can be simulated by semi-random chemical crosslinking. The concentration of the crosslinked protein-enzyme dimer can be accurately determined by the crosslinking/crowding of heme proteins (which allows the accurate measurement of K_M, k_{cat}, and V_{max}).

The results above suggest that the net surface charge of a single protein can have a robust, long-range electrostatic effect on the activity of an enzyme by a salt or ion-mediated mechanism. However, the results of this particular case—the crowding of RNase A by a single subunit of Mb, Cyt c, and S-Cyt c—are by no means general to enzymes or the effect of crowding.

One noted limitation of this methodology is that it currently is capable of crowding one or two proteins around a target protein (i.e., resulting in dimers or trimers). Regarding the ideal, maximum number of proteins that could crowd or contact a central protein at any given time—i.e., the solution to the "kissing number problem" of geometry—it is possible to contact a central sphere with 12 surrounding spheres.[95] The optimization of this current crosslinking method might achieve higher degrees of crowding, that are nearer to this theoretical maximum.

4 | MATERIALS AND METHODS

4.1 | Crosslinking proteins via Staudinger ligation

RNase A, Mb, and Cyt c were purchased from Sigma Aldrich as lyophilized powders and resuspended in 10 mM phosphate buffer, 150 mM NaCl (pH 7.2) to a final concentration of 500 μM. Supercharged Cyt c (denoted S-Cyt c) was prepared by acylation of lysine with succinic anhydride (SA). This modification replaces

the positive charge on lysine with a carboxylic acid (integration of mass spectrum was used to approximate the weighted average number of modifications).[52] Chemical crosslinking of either Mb, Cyt c, or S-Cyt c to RNase A was carried out using NHS-phosphine (i.e., $C_{25}H_{20}NO_6P$ denoted PPh_3, Phos) and NHS-azide (i.e., $C_6H_6N_4O_4$ denoted Az) reagents at molar ratios of 1:5 or 1:3 (protein:linker). The length of the attached Phos linker is 5.4 Å and the Az linker is 2.5 Å (the maximum length of the resulting Staudinger linker is 7.9 Å). Each sample was then reacted at room temperature for 30 min and washed via centrifugal filtration with 20 mM phosphate buffer, 150 mM NaCl (pH 7.2) to remove any excess crosslinker. The resulting proteins modified with NHS-Az or NHS-PPh_3 were then reacted for at least 24 hr at 4°C to form heterodimeric crosslinked proteins.

4.2 | Purification of crosslinked dimers from trimers and monomers

Heterodimeric species were then purified from unreacted monomers or trimers with SEC, using Sephadex G-75 media. The SEC column was run at room temperature using the same linking buffer consisting of 20 mM phosphate, 150 mM NaCl (pH 7.2). Purified heterodimers were verified with SDS-PAGE and MS.

4.3 | Capillary zone electrophoresis

Protein "charge ladders" and CE was used to determine the actual net charge of the proteins as described previously.[52] A Beckman P/ACE MDQ instrument fitted with a silica capillary was used. The capillary was coated with hexadimethrine bromide (polybrene) as previously described.[56] All electrophoresis experiments were conducted at 29 kV in 100 mM sodium acetate (pH 5.0). The capillary was maintained at 22°C via a cooling jacket (to prevent joule heating). Between electrophoresis experiments the capillary was reconditioned via washing with 0.1 M HCl (3 min), methanol (3 min), 0.1 M KOH (3 min), 9.5% w/v polybrene (5 min), and running buffer (5 min). Protein samples were analyzed at a concentration of 150 μm monomer or dimer. Dimethylformamide was added to each sample as a neutral marker of electroosmotic flow.

4.4 | Electrospray ionization MS

The extent of protein modification and crosslinking was measured with electrospray ionization-MS (ESI-MS) using a ThermoFisher™ Discovery Orbitrap mass spectrometer. Protein samples were washed with 0.2% formic acid on a desalting column (Michrom BioResouces, Inc., Auburn CA, USA) to remove excess salt before eluting with an 80:18:2 mixture of acetonitrile, water, and formic acid. Mass spectra were deconvoluted using the MaxEnt1 module in MassLynx software.

4.5 | RNase A assays

Enzyme assays of RNA hydrolysis by RNase A were carried utilizing a modified form of the Kunitz assay.[72] Enzymatic assays of $RNase^{Az}$, RNase–Cyt c, RNase–Mb, or RNase–S-Cyt c were carried out in 1 mM sodium acetate with 10 mM NaCl or 200 mM NaCl (pH 5.01) as well as 1 mM MES with 10 mM NaCl or 200 mM NaCl (pH 6.02). All assays were carried out in 22°C. The RNA substrate that we used for RNase A assays was purchased from Sigma Aldrich. This lyophilized RNA is a polydisperse mixture of total RNA purified from yeast. Briefly, each assay was performed on a Thermo Varioskan LUX Multimode Plate Reader following a decrease in absorbance at 300 nm. Experiments were performed in technical replicates of 24. RNA concentrations varied from either 0.2 to 2.2 or 0.2 to 4.0 mg/ml with a final RNase A concentration of ~0.1 μM (diluted from 1 μM to 0.1 μM). Michaelis–Menten plots were fit to initial velocity vs. substrate concentration (expressed in mg/ml as previously described) to obtain kinetic parameters; K_M, V_{max}, and k_{cat}.

4.6 | Hydrogen/deuterium exchange LC-ESI-MS

H/D exchange was performed as previously described.[47] Briefly, isotopic exchange was initiated by diluting 100 μl of protein (20 μM protein) into 900 μl of 99.9% D_2O (Cambridge Isotope Laboratories, Inc., Tewksbury, MA, USA). H/D exchange was conducted at 22°C. 50 μl aliquots of sample were removed and flash frozen at time points from immediate mixing/dilution up to 60 min following incubation at 22°C. The remaining solution was then placed on a heat block at 90°C for 5 min to produce a perdeuterated sample to quantify back exchange. A sample of 50 μl of this was then flash frozen and stored at −80°C. Mass spectrometric analysis was completed utilizing a ThermoFisher™ Orbitrap Discovery or Thermo Scientific™ Orbitrap Q Exactive™ Focus (S-Cyt c). These samples were then diluted with 950 μl of ice-chilled 2% formic acid. The samples were then immediately loaded on to a desalting column (Michrom BioResouces, Inc.,

Auburn CA, USA) and eluted with an 80:18:2% (v/v) mixture of acetonitrile, water, and formic acid. This desalting apparatus was submerged in ice during each experiment. The mass measurements were made in approximately 3 min from time of thawing (1 min sample preparation, 2 min data collection).

4.7 | Differential scanning calorimetry

The thermostability of S-Cyt c (prepared by acylation of lysine with SA) was measured with DSC as previously described.[66] Briefly, Cyt c and S-Cyt c were washed into linking buffer (10 mM phosphate buffer, 150 mM NaCl pH 7.2). Calorimetry was performed from 20 to 110°C at a scan rate of 1°C/min, using a MicroCal VP-DSC calorimeter (Malvern Instruments). Normalization of protein concentration and baseline corrections were performed on thermograms prior to fitting with a two-state nonbinding model where melting temperature (T_m) were obtained.

4.8 | Identification of chemical modifications with tandem MS of tryptic fragments

Tryptic fragments of each partially acylated protein were generated as follows. Proteins were reduced with dithiothreitol (DTT, 2 mM) at room temperature for 1 hr. Trypsin Gold (Promega®, WI, USA) was added at a molar ratio of 1:20 trypsin to protein and incubated at 37°C for 24 hr in 50 mM Tris–HCl buffer (pH 8.8). Following digestion, each sample (approximately 500 µl in total volume) was lyophilized and then resuspended in 50 µl of reducing buffer (50 mM Tris–HCl, 2 mM DTT). These samples were sequenced with LC/MS/MS (LTQ LX/Orbitrap Q Exactive™ Focus Thermo Scientific™).

Proteomic analysis of MS/MS spectra were performed using SeQuest. Variable modifications of azide (+83.05 Da) and phosphine (+346.31 Da) on lysine residues were queried. Peptide-spectrum matches (PSMs) were validated with false discovery rate confidence thresholds of 0.01–0.05. PSMs of high and medium confidence were considered. PSM filtering also considered the following parameters: Xcorr, ΔCn, and precursor mass accuracy.

AUTHOR CONTRIBUTIONS

Jordan C. Koone: Conceptualization (lead); data curation (lead); formal analysis (lead); investigation (lead); methodology (lead); project administration (lead); validation (lead); visualization (lead); writing – original draft (lead); writing – review and editing (lead). **Chad M. Dashnaw:** Conceptualization (supporting); investigation (supporting); methodology (equal); writing – review and editing (supporting). **Mayte Gonzalez:** Data curation (supporting); formal analysis (supporting); writing – review and editing (supporting). **Bryan F. Shaw:** Conceptualization (equal); funding acquisition (lead); investigation (equal); methodology (equal); project administration (equal); resources (equal); supervision (lead); validation (equal); visualization (equal); writing – original draft (equal); writing – review and editing (equal).

ACKNOWLEDGMENTS

This research was supported by grants from the National Science Foundation (CHE: 2203441) and the Welch Foundation (AA-1854).

CONFLICT OF INTEREST

The authors declare no conflict of interest.

ORCID

Jordan C. Koone https://orcid.org/0000-0003-2021-5298
Bryan F. Shaw https://orcid.org/0000-0001-8265-5833

REFERENCES

1. Warshel A. Energetics of enzyme catalysis. Proc Natl Acad Sci U S A. 1978;75(11):5250–5254.
2. Vascon F, Gasparotto M, Giacomello M, et al. Protein electrostatics: From computational and structural analysis to discovery of functional fingerprints and biotechnological design. Comput Struct Biotechnol J. 2020;18:1774–1789.
3. Roca M, Oliva M, Castillo R, Moliner V, Tunon I. Do dynamic effects play a significant role in enzymatic catalysis? A theoretical analysis of formate dehydrogenase. Chem A Eur J. 2010; 16(37):11399–11411.
4. Adamczyk AJ, Cao J, Kamerlin SC, Warshel A. Catalysis by dihydrofolate reductase and other enzymes arises from electrostatic preorganization, not conformational motions. Proc Natl Acad Sci U S A. 2011;108(34):14115–14120.
5. Krzeminska A, Moliner V, Swiderek K. Dynamic and electrostatic effects on the reaction catalyzed by hiv-1 protease. J Am Chem Soc. 2016;138(50):16283–16298.
6. Warshel A, Sharma PK, Kato M, Xiang Y, Liu H, Olsson MH. Electrostatic basis for enzyme catalysis. Chem Rev. 2006; 106(8):3210–3235.
7. Warshel A, Bora RP. Perspective: Defining and quantifying the role of dynamics in enzyme catalysis. J Chem Phys. 2016; 144(18):180901.
8. Fried SD, Boxer SG. Electric fields and enzyme catalysis. Annu Rev Biochem. 2017;86:387–415.
9. Park C, Raines RT. Quantitative analysis of the effect of salt concentration on enzymatic catalysis. J Am Chem Soc. 2001; 123(46):11472–11479.
10. Gitlin I, Carbeck JD, Whitesides GM. Why are proteins charged? Networks of charge-charge interactions in proteins measured by charge ladders and capillary electrophoresis. Angew Chem Int Ed Engl. 2006;45(19):3022–3060.

11. Rana PS, Kurokawa M, Model MA. Evidence for macromolecular crowding as a direct apoptotic stimulus. J Cell Sci. 2020; 133(9):jcs243931.
12. Gamero-Quijano A, Bhattacharya S, Cazade PA, et al. Modulating the pro- apoptotic activity of cytochrome c at a biomimetic electrified interface. Sci Adv. 2021;7(45):eabg4119.
13. Li P, Banjade S, Cheng HC, et al. Phase transitions in the assembly of multivalent signalling proteins. Nature. 2012; 483(7389):336–340.
14. Park IS, Kim JE. Potassium efflux during apoptosis. J Biochem Mol Biol. 2002;35(1):41–46.
15. Model MA. Possible causes of apoptotic volume decrease: An attempt at quantitative review. Am J Physiol Cell Physiol. 2014; 306(5):C417–C424.
16. Benton LA, Smith AE, Young GB, Pielak GJ. Unexpected effects of macromolecular crowding on protein stability. Biochemistry. 2012;51(49):9773–9775.
17. Wang Y, Sarkar M, Smith AE, Krois AS, Pielak GJ. Macromolecular crowding and protein stability. J Am Chem Soc. 2012; 134(40):16614–16618.
18. Van den Berg B, Ellis RJ, Dobson CM. Effects of macromolecular crowding on protein folding and aggregation. EMBO J. 1999;18(24):6927–6933.
19. Aumiller WM Jr, Davis BW, Hatzakis E, Keating CD. Interactions of macromolecular crowding agents and cosolutes with small-molecule substrates: Effect on horseradish peroxidase activity with two different substrates. J Phys Chem B. 2014; 118(36):10624–10632.
20. del Alamo M, Rivas G, Mateu MG. Effect of macromolecular crowding agents on human immunodeficiency virus type 1 capsid protein assembly in vitro. J Virol. 2005;79(22):14271–14281.
21. Kuznetsova IM, Turoverov KK, Uversky VN. What macromolecular crowding can do to a protein. Int J Mol Sci. 2014;15(12): 23090–23140.
22. Wichert WR, Han D, Bohn PW. Effects of molecular confinement and crowding on horseradish peroxidase kinetics using a nanofluidic gradient mixer. Lab Chip. 2016;16(5):877–883.
23. Ellis RJ. Macromolecular crowding: Obvious but underappreciated. Trends Biochem Sci. 2001;26(10):597–604.
24. Ralston GB. Effects of crowding in protein solutions. J Chem Educ. 1990;67(10):857–860.
25. Nichol LW, Sculley MJ, Ward LD, Winzor DJ. Effects of thermodynamic nonideality in kinetic-studies. Arch Biochem Biophys. 1983;222(2):574–581.
26. Nichol LW, Sculley MJ, Ward LD, Winzor DJ. Enhancement of enzyme-activity by space-filling molecules. Proc Aust Biochem Soc. 1983;15:9.
27. Asaad N, Engberts JBFN. Cytosol-mimetic chemistry: Kinetics of the trypsin- catalyzed hydrolysis of p-nitrophenyl acetate upon addition of polyethylene glycol and n-tert-butyl acetoacetamide. J Am Chem Soc. 2003;125(23):6874–6875.
28. Park C, Raines RT. Catalysis by ribonuclease A is limited by the rate of substrate association. Biochemistry. 2003;42(12): 3509–3518.
29. Raines RT. Ribonuclease A. Chem Rev. 1998;98(3):1045–1066.
30. Park C, Raines RT. Origin of the "inactivation" of ribonuclease A at low salt concentration. FEBS Lett. 2000;468(2–3):199–202.
31. Abdolvahabi A, Gober JL, Mowery RA, Shi Y, Shaw BF. Metal-ion-specific screening of charge effects in protein amide H/D exchange and the Hofmeister series. Anal Chem. 2014;86(20): 10303–10310.
32. Dumetz AC, Snellinger-O'Brien AM, Kaler EW, Lenhoff AM. Patterns of protein protein interactions in salt solutions and implications for protein crystallization. Protein Sci. 2007;16(9): 1867–1877.
33. Jungwirth P, Cremer PS. Beyond Hofmeister. Nat Chem. 2014; 6(4):261–263.
34. Schultz LW, Quirk DJ, Raines RT. His...Asp catalytic dyad of ribonuclease A: Structure and function of the wild-type, D121N, and D121A enzymes. Biochemistry. 1998;37(25):8886–8898.
35. Quirk DJ, Raines RT. His...Asp catalytic dyad of ribonuclease a: Histidine pk_a values in the wild-type, D121N, and D121A enzymes. Biophys J. 1999;76(3):1571–1579.
36. Quirk DJ, Park C, Thompson JE, Raines RT. His...Asp catalytic dyad of ribonuclease A: Conformational stability of the wild-type, D121N, D121A, and H119A enzymes. Biochemistry. 1998; 37(51):17958–17964.
37. Fisher BM, Schultz LW, Raines RT. Coulombic effects of remote subsites on the active site of ribonuclease A. Biochemistry. 1998;37(50):17386–17401.
38. Roberts GC, Dennis EA, Meadows DH, Cohen JS, Jardetzky O. The mechanism of action of ribonuclease. Proc Natl Acad Sci U S A. 1969;62(4):1151–1158.
39. Breslow R, Chapman WH Jr. On the mechanism of action of ribonuclease A: Relevance of enzymatic studies with a p-nitrophenylphosphate ester and a thiophosphate ester. Proc Natl Acad Sci U S A. 1996;93(19):10018–10021.
40. Cuchillo CM, Nogues MV, Raines RT. Bovine pancreatic ribonuclease: Fifty years of the first enzymatic reaction mechanism. Biochemistry. 2011;50(37):7835–7841.
41. Park C, Schultz LW, Raines RT. Contribution of the active site histidine residues of ribonuclease A to nucleic acid binding. Biochemistry. 2001;40(16):4949–4956.
42. del Cardayre SB, Raines RT. A residue to residue hydrogen bond mediates the nucleotide specificity of ribonuclease A. J Mol Biol. 1995;252(3):328–336.
43. Wlodawer A, Svensson LA, Sjolin L, Gilliland GL. Structure of phosphate-free ribonuclease A refined at 1.26 Å. Biochemistry. 1988;27(8):2705–2717.
44. del Cardayre SB, Raines RT. Structural determinants of enzymic processivity. Biochemistry. 1994;33(20):6031–6037.
45. Nolan V, Collin A, Rodriguez C, Perillo MA. Effect of polyethylene glycol-induced molecular crowding on the enzymatic activity and thermal stability of beta-galactosidase from kluyveromyces lactis. J Agric Food Chem. 2020;68(33):8875–8882.
46. Ma B, Nussinov R. Structured crowding and its effects on enzyme catalysis. Top Curr Chem. 2013;337:123–137.
47. Dashnaw CM, Koone JC, Abdolvahabi A, Shaw BF. Measuring how two proteins affect each other's net charge in a crowded environment. Protein Sci. 2021;30:1594–1605.
48. Tang X, Bruce JE. Chemical cross-linking for protein-protein interaction studies. Methods Mol Biol. 2009;492:283–293.
49. Sinz A. Investigation of protein-protein interactions in living cells by chemical crosslinking and mass spectrometry. Anal Bioanal Chem. 2010;397(8):3433–3440.
50. Schilling CI, Jung N, Biskup M, Schepers U, Brase S. Bioconjugation via azide- staudinger ligation: An overview. Chem Soc Rev. 2011;40(9):4840–4871.

51. Sinz A. Chemical cross-linking and mass spectrometry to map three-dimensional protein structures and protein-protein interactions. Mass Spectrom Rev. 2006;25(4):663–682.
52. Colton IJ, Anderson JR, Gao JM, Chapman RG, Isaacs L, Whitesides GM. Formation of protein charge ladders by acylation of amino groups on proteins. J Am Chem Soc. 1997; 119(52):12701–12709.
53. van Berkel SS, van Eldijk MB, van Hest JC. Staudinger ligation as a method for bioconjugation. Angew Chem Int Ed Engl. 2011;50(38):8806–8827.
54. Kang K, Choi JM, Fox JM, Snyder PW, Moustakas DT, Whitesides GM. Acetylation of surface lysine groups of a protein alters the organization and composition of its crystal contacts. J Phys Chem B. 2016;120(27):6461–6468.
55. Shaw BF, Schneider GF, Bilgicer B, et al. Lysine acetylation can generate highly charged enzymes with increased resistance toward irreversible inactivation. Protein Sci. 2008;17(8):1446–1455.
56. Zahler CT, Zhou HY, Abdolvahabi A, et al. Direct measurement of charge regulation in metalloprotein electron transfer. Angew Chem Int Ed. 2018;57(19):5364–5368.
57. Lund M, Jonsson B. Charge regulation in biomolecular solution. Q Rev Biophys. 2013;46(3):265–281.
58. Bakhshandeh A, Frydel D, Levin Y. Charge regulation of colloidal particles in aqueous solutions. Phys Chem Chem Phys. 2020;22(42):24712–24728.
59. Zhang Z, Witham S, Alexov E. On the role of electrostatics in protein-protein interactions. Phys Biol. 2011;8(3):035001.
60. Palmadottir T, Malmendal A, Leiding T, Lund M, Linse S. Charge regulation during amyloid formation of alpha-synuclein. J Am Chem Soc. 2021;143(20):7777–7791.
61. Lund M, Jonsson B. On the charge regulation of proteins. Biochemistry. 2005;44(15):5722–5727.
62. Hyman AA, Weber CA, Julicher F. Liquid-liquid phase separation in biology. Annu Rev Cell Dev Biol. 2014;30:39–58.
63. Zhou HX, Pang XD. Electrostatic interactions in protein structure, folding, binding, and condensation. Chem Rev. 2018; 118(4):1691–1741.
64. Baumer KM, Cook CD, Zahler CT, et al. Supercharging prions via amyloid-selective lysine acetylation. Angew Chem Int Ed Engl. 2021;60(27):15069–15079.
65. Abdolvahabi A, Shi Y, Rhodes NR, Cook NP, Marti AA, Shaw BF. Arresting amyloid with coulomb's law: Acetylation of ALS-linked SOD1 by aspirin impedes aggregation. Biophys J. 2015;108(5):1199–1212.
66. Rasouli S, Abdolvahabi A, Croom CM, et al. Lysine acylation in superoxide dismutase-1 electrostatically inhibits formation of fibrils with prion-like seeding. J Biol Chem. 2017;292(47): 19366–19380.
67. Shaw BF, Schneider GF, Arthanari H, et al. Complexes of native ubiquitin and dodecyl sulfate illustrate the nature of hydrophobic and electrostatic interactions in the binding of proteins and surfactants. J Am Chem Soc. 2011;133(44):17681–17695.
68. Shaw BF, Arthanari H, Narovlyansky M, et al. Neutralizing positive charges at the surface of a protein lowers its rate of amide hydrogen exchange without altering its structure or increasing its thermostability. J Am Chem Soc. 2010;132(49): 17411–17425.
69. Shi Y, Mowery RA, Shaw BF. Effect of metal loading and subcellular pH on net charge of superoxide dismutase-1. J Mol Biol. 2013;425(22):4388–4404.
70. Hamuro Y. Determination of equine cytochrome c backbone amide hydrogen/deuterium exchange rates by mass spectrometry using a wider time window and isotope envelope. J Am Soc Mass Spectrom. 2017;28(3):486–497.
71. Bagel'ova J, Antalik M, Tomori Z. Effect of polyglutamate on the thermal stability of ferricytochrome c. Biochem Mol Biol Int. 1997;43(4):891–900.
72. Kunitz M. A spectrophotometric method for the measurement of ribonuclease activity. J Biol Chem. 1946;164(2):563–568.
73. Selles B, Zannini F, Couturier J, Jacquot JP, Rouhier N. Atypical protein disulfide isomerases (pdi): Comparison of the molecular and catalytic properties of poplar pdi-a and pdi-m with pdi-l1a. PLoS One. 2017;12(3):e0174753.
74. Margoliash E, Frohwirt N. Spectrum of horse-heart cytochrome c. Biochem J. 1959;71(3):570–572.
75. Millar SJ, Moss BW, Stevenson MH. Some observations on the absorption spectra of various myoglobin derivatives found in meat. Meat Sci. 1996;42(3):277–288.
76. Smith BD, Soellner MB, Raines RT. Potent inhibition of ribonuclease a by oligo(vinylsulfonic acid). J Biol Chem. 2003; 278(23):20934–20938.
77. Thompson JE, Kutateladze TG, Schuster MC, Venegas FD, Messmore JM, Raines RT. Limits to catalysis by ribonuclease A. Bioorg Chem. 1995;23(4):471–481.
78. James DA, Burns DC, Woolley GA. Kinetic characterization of ribonuclease S mutants containing photoisomerizable phenylazophenylalanine residues. Protein Eng. 2001;14(12): 983–991.
79. Messmore JM, Raines RT. Decavanadate inhibits catalysis by ribonuclease A. Arch Biochem Biophys. 2000;381(1):25–30.
80. Lopez-Alonso JP, Bruix M, Font J, et al. Nmr spectroscopy reveals that Rnase a is chiefly denatured in 40% acetic acid: Implications for oligomer formation by 3d domain swapping. J Am Chem Soc. 2010;132(5):1621–1630.
81. Campbell FE, Cassano AG, Anderson VE, Harris ME. Pre-steady-state and stopped- flow fluorescence analysis of escherichia coli ribonuclease iii: Insights into mechanism and conformational changes associated with binding and catalysis. J Mol Biol. 2002;317(1):21–40.
82. Phillips CM, Mizutani Y, Hochstrasser RM. Ultrafast thermally-induced unfolding of Rnase-a. Proc Natl Acad Sci U S A. 1995;92(16):7292–7296.
83. Eberhardt ES, Wittmayer PK, Templer BM, Raines RT. Contribution of a tyrosine side chain to ribonuclease A catalysis and stability. Protein Sci. 1996;5(8):1697–1703.
84. Beach H, Cole R, Gill ML, Loria JP. Conservation of mu s-ms enzyme motions in the apo- and substrate-mimicked state. J Am Chem Soc. 2005;127(25):9167–9176.
85. Montioli R, Campagnari R, Fasoli S, et al. Rnase a domain-swapped dimers produced through different methods: Structure-catalytic properties and antitumor activity. Life (Basel). 2021;11(2):168.
86. Gotte G, Bertoldi M, Libonati M. Structural versatility of bovine ribonuclease A. Distinct conformers of trimeric and tetrameric aggregates of the enzyme. Eur J Biochem. 1999; 265(2):680–687.

87. Messmore JM, Fuchs DN, Raines RT. Ribonuclease A: Revealing structure-function relationships with semisynthesis. J Am Chem Soc. 1995;117(31):8057–8060.
88. Trautwein K, Holliger P, Stackhouse J, Benner SA. Site-directed mutagenesis of bovine pancreatic ribonuclease: Lysine-41 and aspartate-121. FEBS Lett. 1991;281(1–2):275–277.
89. Lu WP, Fei L. A logarithmic approximation to initial rates of enzyme reactions. Anal Biochem. 2003;316(1):58–65.
90. Perrin CL. Linear or nonlinear least-squares analysis of kinetic data? J Chem Educ. 2017;94(6):669–672.
91. Ramos CH, Baldwin RL. Sulfate anion stabilization of native ribonuclease A both by anion binding and by the Hofmeister effect. Protein Sci. 2002;11(7):1771–1778.
92. Sotomayor-Perez AC, Karst JC, Ladant D, Chenal A. Mean net charge of intrinsically disordered proteins: Experimental determination of protein valence by electrophoretic mobility measurements. Methods Mol Biol. 2012;896:331–349.
93. Gokarn YR, Fesinmeyer RM, Saluja A, et al. Effective charge measurements reveal selective and preferential accumulation of anions, but not cations, at the protein surface in dilute salt solutions. Protein Sci. 2011;20(3):580–587.
94. Pokorna J, Heyda J, Konvalinka J. Ion specific effects of alkali cations on the catalytic activity of hiv-1 protease. Faraday Discuss. 2013;160:359–370.
95. Kucherenko S, Belotti P, Liberti L, Maculan N. New formulations for the kissing number problem. Discrete Appl Math. 2007;155(14):1837–1841.

SUPPORTING INFORMATION

Additional supporting information can be found online in the Supporting Information section at the end of this article.

How to cite this article: Koone JC, Dashnaw CM, Gonzalez M, Shaw BF. A method for quantifying how the activity of an enzyme is affected by the net charge of its nearest crowded neighbor. Protein Science. 2022;31(9):e4384. https://doi.org/10.1002/pro.4384